

**IDETC2022-89164**

## **A STUDY OF MACHINE LEARNING FRAMEWORK FOR ENABLING EARLY DEFECT DETECTION IN WIRE ARC ADDITIVE MANUFACTURING PROCESSES**

**Nowrin Akter Surovi**

Engineering Product Development  
Singapore University of  
Technology and Design  
Singapore 487372

Email: surovi.akter@mymail.sutd.edu.sg

**Shaista Hussain**

Institute of High Performance Computing  
Agency for Science, Technology  
and Research (A\*STAR)  
Singapore 138632

Email: hussains@ihpc.a-star.edu.sg

**Gim Song Soh**

Engineering Product Development  
Singapore University of  
Technology and Design  
Singapore 487372

Email: sohgimsong@sutd.edu.sg

### **ABSTRACT**

*This paper presents the study on the performance of a variety of proposed time-domain acoustic features-based frameworks for the detection of geometrically defective print segments during the Wire Arc Additive Manufacturing (WAAM) process. Specifically, we investigate into a variety of acoustic features, namely the Root Mean Square of Pressure (RMSP), Energy, Mean Amplitude, Kurtosis, Zero Crossing Rate (ZCR), Skewness, Crest Factor and Peak-to-peak, and print process parameters, namely Torch Speed (TS) and Wire Feed Rate (WFR) combined with Machine Learning (ML) frameworks for detecting geometrically defective print segments. Experiments carried out on Inconel 718 show that among the studied frameworks, using acoustic features and process parameters with Random Forest (RF) performs best in terms of F1 score at 89%, while using acoustic features and process parameters with Support Vector Machine (SVM) performs best in picking out defective segments based on the Confusion Matrix. These findings serve as our first step in developing an intelligent sensing system for the early identification of defective beads in the WAAM printing process, so that appropriate intervention can be implemented to save printing resources and material costs. In addition, the proposed approach has the advantage of detecting defects within a more localized region for more targeted intervention.*

### **1 INTRODUCTION**

Wire Arc Additive Manufacturing (WAAM) is an arc-welding-based additive manufacturing technique that uses wire as a feedstock to build 3D metallic components by depositing weld beads in a layer-by-layer fashion. Recently, WAAM is becoming popular in the metal manufacturing industry because of its low equipment cost, low buy-to-fly ratio, high deposition rate, and friendly to the environment [1–4]. During the printing process, assurance of its resulting print quality is a challenging task because different types of defects, such as lack of fusion, porosity, cracks, distortion, oxidation, etc., can occur during the printing process. These reduce the strength of the final printed product, thus affecting its lifespan and performance. Hence, it is important to identify the defective printing process early so that appropriate corrective measures can be taken during the printing process to save printing resources and material costs. In this paper, we focus on detecting geometric defects because having geometric defects in one layer contribute to voids or porosity within the part itself, thus affecting its strength and quality. See Figure 1.

In the literature, numerous techniques have been employed to sense defects. This included inferring it from acoustic signals, X-ray radiation, image, thermal measurement, etc. [1]. Among these, acoustic sensors have several advantages over other measurement techniques due to their low cost, ease of maintenance, radiation-free, and portability. The acoustic sound generated by

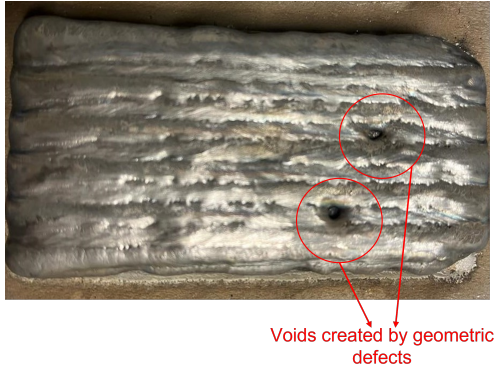


**FIGURE 1:** Geometrically defective segments lead to voids between two successive beads will affect the final printed part strength and quality.

the electric arc comes from the pulsation of the electric arc and the vibration of the weld pool metal [5]. Several works explored the relationships between the geometry of beads and the properties of acoustic signals [6]. Polajnar et al. [7] showed that irregularities in the bead geometry are reflected in the intensity of acoustic signals. Pal et al. [8] showed that acoustic signals could identify metal transfer mode and weld defects. Lv et al. [9] showed that the height of the arcs constituting the shape of the bead has a linear relationship with the pressure of the acoustic signal. Due to the relationships mentioned above between the properties of the bead geometry and the measured acoustic signals inspires us to extract and use acoustic features to capture the geometric defects during the WAAM process with appropriate feature-based models.

Acoustic features and acoustic feature-based models have been used in domains ranging from food science to voice recognition and medical diagnostics to solve various domain-specific classification problems. For example, in the domain of food science and technology, Zhao et al. [10] extracted features from the time-domain acoustic signal and applied Principal Component Analysis (PCA) to determine eggshell crack. In the voice pattern recognition problem, Che Yong et al. [11] used acoustic features to develop an animal voice identification (ID) detection system. In the medical domain, Bradley M Whitaker et al. [12] used time-domain features and Support Vector Machine (SVM) for the classification of different heart sounds. Encouraged by the success of acoustic features and acoustic feature-based models in the above domains, our goal here seek to extend this into the additive manufacturing domain through the use of acoustic signal-based framework for identifying defective segments of beads.

In this paper, we proposed a variety of new defect detection frameworks and comparatively evaluated its performance and benchmark with our previous study [13] based on Inconel 718 material. Specifically, we investigate into a variety of acous-

tic features and print process parameters combined with Machine Learning (ML) frameworks for detecting geometrically defective print segments. The difference between our previous work and the present work is threefold. Firstly, in our previous paper, we explored detection frameworks that use frequency-domain features only, whereas here, we explored detection frameworks that use time-domain features. Secondly, in our previous paper, we identified defective beads as a whole, whereas here, we increased its resolution and identified defective segments of a bead so that earlier detection and targeted intervention can be possible. Lastly, in the present paper, we explore the incorporation of machine process parameters which was not explored previously.

## 2 EXPERIMENTAL SETUP AND DATA COLLECTION

In this section, we explain our experimental setup, data collection, and dataset labelling approach.

### 2.1 Experimental Setup

The experiments were conducted on our robotic WAAM system at Singapore University of technology and Design (SUTD), as shown in Figure 2.

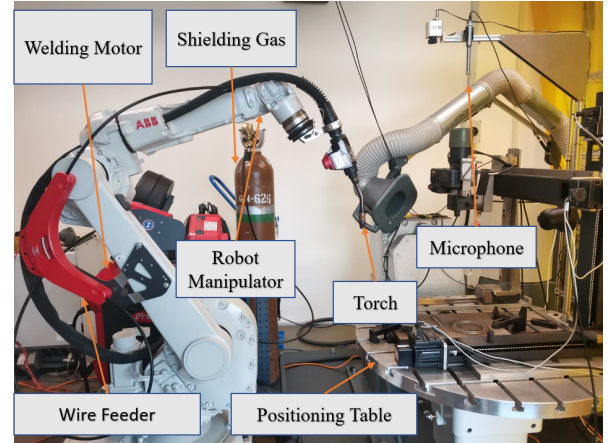


**FIGURE 2:** Experimental setup of SUTD Robotic WAAM for Bead Printing and Acoustic Data Collection

The system consists of a robot manipulator (ABB IRB1660ID), a welding power source (Fronius TPS 400i) equipped with a welding torch (Fronius WF 25i Robacta Drive), a cartesian coordinate robot made up of three linear rails (PMI KM4510) powered by three servos (SmartMotor SM34165DT), a 2D laser scanner (Micro-Epsilon scanCONTROL 2910-100) and a microphone (UMIK-1 miniDSP) installed at around 80 cm above the substrate in order to minimize environmental noise.

## 2.2 Data Collection

We printed 23 weld beads from Inconel 718 wires (BÖHLER 3Dprint AM 718) using different combinations of torch speed and wire feed rate to obtain different weld bead geometries. The torch speed and wire feed rate were in the range of 1-12 mm/s and 2-8 m/min, respectively. We collected the corresponding acoustic signals at 44 kHz, and then we segmented each bead signal into ten signal segments. Thus, we get two hundred thirty signal segments for different torch speeds and wire feed rates. Since the different combinations of torch speed and wire feed rate produce different lengths of the acoustic signals, we use the downsampling [13] approach to make all the acoustic signal segments of the same length with the same sampling rate. After this preprocessing, the duration of each acoustic signal segment is around 0.5 s.

## 2.3 Dataset Labelling

Our objective is to identify geometrically defective segments of beads. To train our frameworks to identify defective segments, we need to assign labels to the signal segments based on which the ML model can learn to make decisions. Hence we label each of the signal segments in the Inconel data sets. In our previous paper, we labeled all the signal segments of a non-defective bead as “good” and all the signal segments of a defective bead as “bad” because we consider the whole bead as defective or non-defective [13]. However, in this paper, we assign different labels to different signal segments of a bead. In this manner, we have labelled around 25% signal segments as bad and 75% signal segments as good.

In order to label signal segments, we first collected point cloud data of beads using the GOM ATOS III Triple scanner. Then we divided the whole bead point cloud data into ten segments of an equal number of points. Then we determine the range of Gaussian curvature of each of the bead segments. We categorized all the bead segments into good and bad based on different thresholds of range curvature. The distributions of range curvature values for good and bad segments were plotted for each choice of threshold. Finally, we set a threshold for good and bad segments when the overlapping region of the two distribution plots is minimum, as shown in Figure 3. In the Figure, the x-axis represents the values of range curvature of segmented beads, and the y-axis represents the probability density estimate of each variable. Therefore, we select 0.3 mm as threshold that can be used for the detection of defective bead segments. A bead segment with a range curvature below the threshold is considered a non-defective segment. The bead segment with a range curvature higher than the threshold is considered a defective segment.

Examples of geometrically defective and non-defective segments and their corresponding acoustic waveforms are shown in Figure 4.

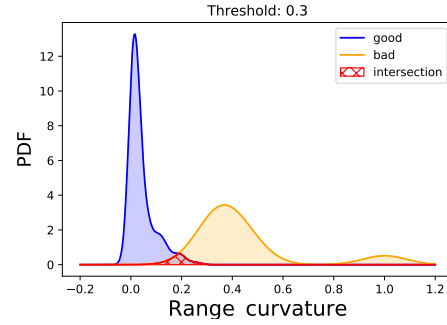


**FIGURE 3:** Threshold selection distribution plot

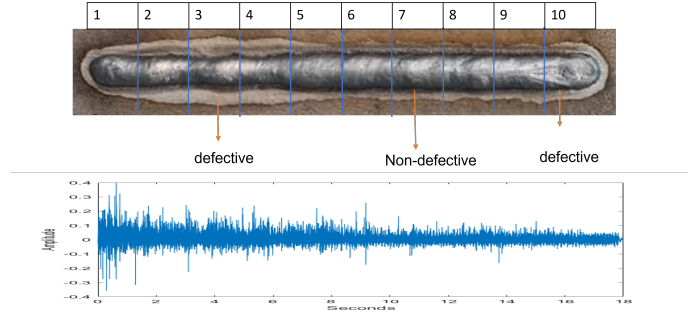


**FIGURE 4:** Geometrically defective and non-defective segments with acoustic time-domain waveforms.

## 3 DESCRIPTION OF THE FEATURES AND ML MODELS

In this section, we explain the various features and ML models used for the detection of geometrically defective bead segments. Our proposed workflow is as shown in Figure 5. It be-

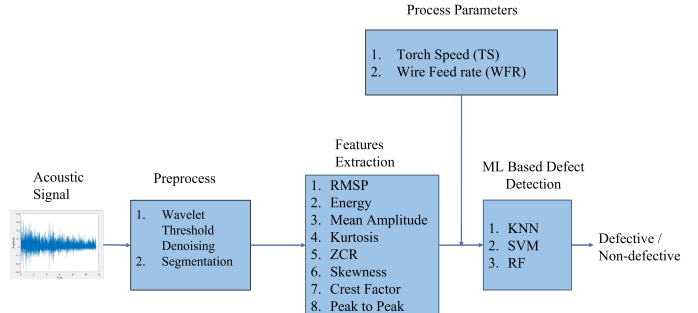


**FIGURE 5:** Our proposed workflow for identification of defective segments of beads

gins with pre-processing (See Section 2.2), followed by feature extraction, and then by ML-based defect detection. In the fol-

lowing, we explain the acoustic features and process parameters used and the three ML-based models for defect identification.

### 3.1 Acoustic Features

The eight acoustic signatures used in this study are RMSP, Energy, Mean Amplitude, Kurtosis, ZCR, Skewness, Crest Factor, and Peak-to-peak. Their specifics are explained as follows:

**3.1.1 RMSP** The root mean square pressure (RMSP) is the root of the mean of the squared pressure of the sound signal over a time duration. The RMSP is most often used to characterize a sound wave because it is directly related to the energy carried by the sound wave [14]. The RMSP of a signal in a time from 0 to T is given by:

$$P = \sqrt{\frac{1}{T} \int_{i=0}^T p^2(t) dt} \quad (1)$$

$p(t)$  is the instantaneous pressure. The RMSP is an important factor in arc sound. It indicates the metal transfer modes in WAAM [8].

**3.1.2 Energy** Energy of sound is a general method of analyzing the acoustic signal in the time domain. It is used in different domains such as analyzing the animal population and recognizing the music instrument [15], and so on. The energy of sound is expressed using the following equation:

$$E = \sum_{i=1}^N x_i^2(n) \quad (2)$$

$N$  is the number of samples taken within the time domain signal  $x(n)$ . The arc sound transmits energy into a medium through its vibration. It is commonly used for monitoring the WAAM process [16]. Too high arc sound energy indicates the possibility of defects [17].

**3.1.3 Mean Amplitude** The amplitude of a sound signal is a statistical feature of sound that determines the loudness of the sound. A larger amplitude means a louder sound, and a smaller amplitude means a softer sound. The mean amplitude of a signal be expressed as

$$A = \frac{1}{N} \sum_{i=1}^N |x_i| \quad (3)$$

A perfect weld usually has a uniform amplitude in its sound signals. Sound peaks with larger than normal amplitudes may point

to possible defects in the weld. The welding process is said to be good if sound signals have similar amplitudes within the time intervals. [18].

**3.1.4 Kurtosis** Kurtosis is used to analyze the vibratory amplitudes' distribution in a time-domain signal. Kurtosis is expressed by the following equation:

$$y = \frac{\frac{1}{N} \sum_{i=1}^N (x_i - \bar{x})^4}{\sigma^4} \quad (4)$$

It indicates the degree of sharpness, metal transfer mode, peak status, and steep level of arc sound signal [19, 20]. From the literature [8, 20], it is concluded that the arc sound kurtosis is a good indicator of the weld defect; however, the accuracy of the defect detection with sound kurtosis was not studied.

**3.1.5 ZCR** ZCR (Zero Crossing Rate) is the number of times the sound signal changes its sign. ZCR helps to estimate the fundamental frequency of speech for speech processing applications [15]. It is also helpful for discriminating speech from noise and for determining the start and end of speech segments [21]. ZCR can be expressed as:

$$ZCR = \frac{f}{N} \sum_{i=1}^N |sgn(x(n)) - sgn(x(n-1))| \quad (5)$$

where

$$|sgn(x(n))| = \begin{cases} +1 & \text{if } x(n) > 0 \\ -1 & \text{if } x(n) < 0 \end{cases} \quad (6)$$

$f$  is the sampling rate of signal. ZCR detects the variation of arc sound from its ideal arc behavior during welding [22].

**3.1.6 Skewness** The skewness factor is also an important factor in the processing of signals. It is expressed as

$$SK = \frac{1}{N} \sum_{i=1}^N \left( \frac{x_i - \bar{x}}{\sigma} \right)^3 \quad (7)$$

It is used to distinguish different transfer modes [23] and different penetration states of the welding pool [24].

**3.1.7 Crest Factor** Crest factor (CF) is a statistical parameter of sound signal that corresponds to the ratio of maximum value and RMS value of a signal.

$$CF = \frac{\max |x_i|}{\sqrt{\frac{1}{N} \sum_{i=1}^N x_i^2}} \quad (8)$$

It is used to monitor the impulses in time domain vibration due to the defect in the welding zone. In addition, it is used to compare the welding process for defect-free and defective welds [20].

**3.1.8 Peak-to-Peak** Peak-to-peak (pk-pk) is the difference between the maximum and the minimum amplitudes of a sound signal. It is a characteristic property of sound that is generally used for statistical analysis of sound label [25]. It can be expressed as:

$$y = \max(x) - \min(x) \quad (9)$$

The consistency of the peak-to-peak distance of arc sound indicates a good welding process along the entire welding path. In other words, sound peaks of stable welding should demonstrate a fairly constant pattern.

## 3.2 Process Parameters

In WAAM processes, several key input factors should be assigned before printing in order to get different geometry beads. These parameters such as torch speed, wire feed speed, working distance, arc voltage, deposition strategy or path planning, etc. [26] are called process parameters [13]. Earlier studies have looked at the effects of process parameters such as wire feed rate (WFR) and torch speed (TS) on welding quality, weld-bead geometry [27, 28] and welding defects. It was found that TS and WFR had a major influence on deposition width and height and a stable deposited layer. As TS increased, the deposited layer became worse, and defects started to occur due to lower input heat [29]. Again, surface roughness can be predicted by using process parameters [30]. In general, increasing WFR increases surface roughness. A lower WFR with lower TS decreases the surface roughness [31].

The effect of process parameters on the welding geometry and defects influenced us to use the process parameters as auxiliary features to improve the performance of ML frameworks for defect detection.

## 3.3 ML Model for Defect Identification

In this section, we explain three ML-based models explored for defect identification: KNN, SVM, and RF.

**K-Nearest Neighbors (KNN)** KNN is a supervised learning technique. The algorithm selects  $K$  nearest points of a new sample by calculating the distance among all existing samples with the new sample. The  $K$  nearest neighbors are determined by the shortest distance from the new sample. The class of a new sample is assigned to the majority class of  $K$  nearest points [32]. For this application, we find  $K = 3$  (3 nearest neighbors) is ideal for our frameworks (see Section 4.1).

**Support Vector Machine (SVM)** SVM is a discriminative classifier that creates a line or a hyper-plane to separate data points into different classes. In the present work, a non-linear SVM was trained to classify the bead segments into good and bad based on their input features and corresponding labels. The goal of SVM is to search a function  $f(x)$  with parameters  $\alpha_i$  and  $b$  [33] which can predict defective segments of beads. A general format of SVM is shown as

$$f(x) = \sum_{i=1}^n y_i \alpha_i k(x_i, x) + b$$

Here, we use RBF (radial basis function) kernel  $k(x_i, x) = \exp(-\gamma \|x - x_i\|^2)$ . For our application, we find  $\gamma = 0.1$  ideal for training our frameworks (see Section 4.1).

**Random Forest (RF)** RF is a supervised ML technique that consists of many decision trees as its building blocks. RF is suitable for modeling non-linear and complex systems [29]. It is generally not affected by outliers and noise and involves a faster training process. RF learns to build the relationships between the inputs and outputs in the training stage. Once the training is done, a new example is presented for testing. Each tree in the trained RF then votes for classification [34]. The class with the most votes is used as the predicted class. In our application, we use RF to detect defects in a bead. We find number of trees=100 is suitable for our application (see Section 4.1).

## 4 EXPERIMENTAL RESULTS AND DISCUSSION

In this section, we report and evaluate the training mechanisms (Section 4.1), performance (Section 4.2 and Section 4.3) of our proposed framework based on two types of features. One is based on “Acoustic only”, where we consider features of acoustic signatures only. The second consists of the fusion of both “Acoustic and process parameters”, where we consider both acoustic signatures and process parameters as features. Subsequently, we evaluate three ML models, described above, on their performance to identify defective segments based on these two types of features.

#### 4.1 Training Mechanism

In the following, we discuss the choice of hyperparameters for the purpose of demonstrating the reproducibility of our work for other empirical studies.

**Hyperparameters for KNN** In order to find the optimal  $K$  value required to train the KNN, we obtained the resulting classification error over a range of  $K$ . For each feature type (Acoustic only or Acoustic with process parameters combined), we performed five-fold cross-validation (CV). Then, we calculated the classification error on the training data for each fold as  $K$  varies from  $K = 1, \dots, 50$ . Finally, we computed the average error across the CV folds with respect to different  $K$  values and selected the  $K$  value corresponding to the lowest classification error on the training data as the optimal  $K$  value. The classification error results for the acoustic only, and acoustic and process parameters combined for each  $K$  value, are as shown in the left and right of Figure 6 respectively. Notice that from these five-fold

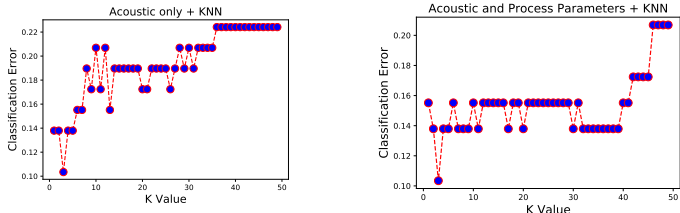


**FIGURE 6:** KNN classification error for each  $K$  value for acoustic features only (left plot) and acoustic and process parameters features combined (right plot)

CV experiments, we find that the lowest mean training classification error is around 0.1 for both acoustic features only, and acoustic features and process parameters combined, which occur at  $K = 3$ . Therefore, we chose  $K = 3$  for the training of both of these feature types.

**Hyperparameters for SVM** Similarly, in order to find a suitable SVM parameter  $\gamma$ , we studied the resulting classification error over a range of  $\gamma$ . Same as before, we performed five-fold CV for each feature type (Acoustic only or Acoustic with process parameters combined). Then we calculated the training classification error as  $\gamma$  varies from  $\gamma = 0.01 \dots 0.5$ . Finally, we obtained the mean training classification error across five folds for each value of  $\gamma$ , and selected the  $\gamma$  that corresponds to the lowest classification error as the optimal  $\gamma$  for training. The results of the classification error are as shown in Figure 7. We find that the lowest mean training classification error is around 0.15 and 0.1 for acoustic features only, and acoustic features and process parameters combined respectively at  $\gamma = 0.1$ . Hence we chose  $\gamma = 0.1$  for the training of both of these features.

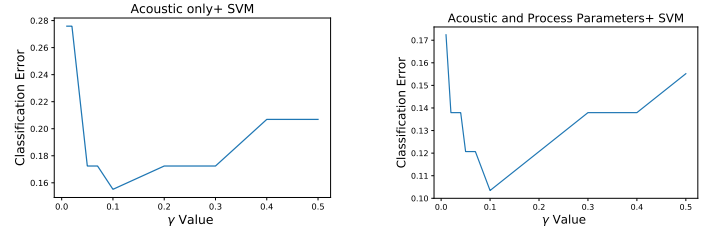


**FIGURE 7:** SVM classification error for each  $\gamma$  value for acoustic features only (left plot) and acoustic and process parameters features combined (right plot)

**Hyperparameters for RF** To find the best number of trees for the RF model, we performed similar five-fold CV experiments as for KNN and SVM models. The number of trees was varied from 1 to 250 to obtain the optimal number of trees based on the lowest training classification error. Figure 8 shows the resulting classification error plot for both feature types. For RF, we find that

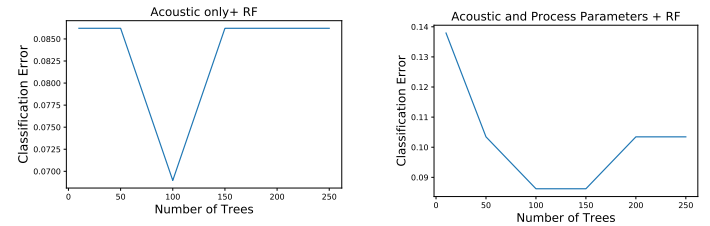


**FIGURE 8:** RF classification error for each number of trees for acoustic features only (left plot) and acoustic and process parameters features combined (right plot)

the lowest mean training classification error is around 0.07 and 0.08 for acoustic features only, and acoustic features and process parameters combined respectively at the number of trees=100. Hence, we chose the number of trees as 100 for training of both these feature types.

#### 4.2 Performance Evaluation Based on F1 Score

In this section, we evaluate the performance of the proposed geometric defect detection frameworks based on the F1 score, which is computed from its precision and recall. The reasons to measure these metrics are two-fold. First, it serves as a quality assessment for a framework with an imbalanced dataset. Second, it allows us to check the performance of a particular geometric defect detection framework.

**Acoustic only + KNN** For training this framework, we add all time-domain features together and use five-fold cross validation [35] to train KNN ( $K=3$ ) model to detect defective segments. Therefore, for training each fold, 184 signal segments are used

for training and 46 signal segments are used for testing. After completing the full training procedure, we get mean F1 score of around 80% based on testing dataset.

**Acoustic only + SVM** Similarly, we add all time-domain features together and use SVM ( $\gamma = 0.1$ ) to detect defective segments. We also use five-fold cross validation for training this framework. After training, we get mean testing F1 score of around 83%.

**Acoustic only + RF** Same as before, for training this framework, we add all time-domain features together and use an RF-based identifier (number of trees=100) to detect defective segments. We use five-fold cross validation for training this framework. After training, we get mean testing F1 score of around 84%.

**Acoustic and process parameters + KNN** For training of this framework, we add all time-domain features and two process parameters together and use KNN ( $K = 3$ ) identifier to detect defective segments. After training, We get mean testing F1 score of around 85%.

**Acoustic and process parameters + SVM** Similarly, we add all time-domain features and process parameters together and use five-fold cross validation for training SVM. After training, we get mean testing F1 score of around 87%.

**Acoustic and process parameters + RF** Same as before, after adding all time-domain features and two process parameters together, we use RF identifier to detect defective segments using five-fold cross validation. After training, we get mean testing F1 score of around 89%.

**Summary** Table 1 shows the summary of our comparative study of the various frameworks combinations. It also shows the comparison with our previously studied best performing frequency domain-based geometric defect detection framework PCA+KNN [13] based on the printing of Inconel material. From the table, it can be seen that all of our existing studied frameworks outperform our previous results [13]. Moreover, we found that the best performing framework based on the F1 score is acoustic features with process parameters trained using RF. This achieves around 89% mean F1 score, about 9% more than our previously studied PCA+KNN framework.

#### 4.3 Performance Evaluation based on Confusion Matrix

From section 4.2, we concluded from the F1 scores that our acoustic and process parameters + RF framework is able to pick out good and bad bead segments more effectively than the other

**TABLE 1:** COMPARATIVE STUDY OF ALL FRAMEWORKS BASED ON TEST DATASET

Framework	F1- Score	Precision	Recall
Acoustic only +KNN	$80.54 \pm 0.06$	$80.76 \pm 0.09$	$80.24 \pm 0.05$
Acoustic only +SVM	$83.50 \pm 0.05$	$84.79 \pm 0.07$	$82.00 \pm 0.06$
Acoustic only +RF	$84.27 \pm 0.03$	$85.58 \pm 0.06$	$84.01 \pm 0.07$
PCA+KNN	$80.09 \pm 0.07$	$86.58 \pm 0.06$	$77.74 \pm 0.07$
Acoustic and process parameters +KNN	$85.48 \pm 0.03$	$85.64 \pm 0.06$	$85.20 \pm 0.02$
Acoustic and process parameters +SVM	$87.50 \pm 0.04$	$86.90 \pm 0.08$	$88.01 \pm 0.07$
Acoustic and process parameters +RF	$89.11 \pm 0.08$	$91.11 \pm 0.01$	$88.96 \pm 0.10$

studied frameworks. However, as our ultimate goal is to identify defective segments of beads, we seek to understand which of these studied frameworks can detect bad segments more accurately in this section.

In order to find which frameworks can accurately classify more bad segments, we utilized confusion matrix [36] as they give information about the predicted and true classification of the good and bad segments. To calculate the confusion matrix, we use five-fold cross-validation approach for each of the frameworks studied, as shown in Table 2. First, we observe that our studied frameworks can effectively pick out good and bad segments compared with our previously explored PCA+KNN approach [13]. We also observed that having both acoustic features and process parameters based framework is able to pick out more bad segments than the acoustic-only framework. Next, we notice that the acoustic features and process parameters with SVM can pick out 43 bad segments of a list of 51 bad segments. In contrast, our previously identified best framework PCA+KNN can pick out only 30 bad segments. Interesting, the best performing framework based on the F1 score (acoustic and process parameters with RF) is not the best framework for identifying bad segments based on its confusion matrix. Because the higher F1 score in acoustic features and process parameters with RF is dominated

by the number of good segments. Therefore, if the objective is to pick out more bad segments accurately, using acoustic and process parameters with SVM is more accurate.

We also analyzed the importance of features based on the mean decrease in impurity. We used the RF model to generate feature importance scores for the acoustic features-based model and acoustic features and process parameters-based model in order to identify which features are most important for predicting the defective segments.

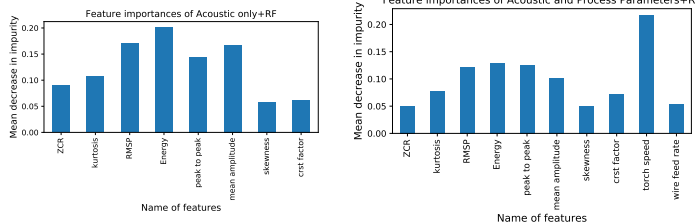


**FIGURE 9:** Impurity based importance calculation for acoustic features only (left plot) and acoustic and process parameters features combined (right plot) using RF model

From Figure 9, we observe that energy, RMSP, mean amplitude, and peak-to-peak features contribute a lot to detect bad segments for the acoustic features only based RF model. Therefore, these features are important for prediction. Again, the acoustic and process parameters features combined plot shows that the torch speed feature significantly influences prediction. Moreover, energy, RMSP, mean amplitude, and peak-to-peak features also have significant contributions in this case.

## 5 CONCLUSION

In this paper, we have explored the use of a variety of time-domain arc sound signatures, namely the Root Mean Square of Pressure (RMSP), Energy, Mean Amplitude, Kurtosis, Zero Crossing Rate (ZCR), Skewness, Crest Factor and Peak-to-peak, and as well as print process parameters, namely the Torch Speed (TS) and Wire Feed Rate (WFR) as features for ML models for the detection of defective print segments during the WAAM process. We have demonstrated the effectiveness of the use of these features based on three ML models: i) K-Nearest Neighbors (KNN); ii) Support Vector Machine (SVM); and iii) Random Forest (RF) for the identification of geometrically defective print segments on Inconel 718. We showed that the performance of the defect detection framework generally increases when we combine both the sound signatures and process parameters, and when these features used in conjunction with SVM, they are the most effective framework in picking out bad segments.

**TABLE 2:** COMPARATIVE STUDY OF CONFUSION MATRICES OF ALL FRAMEWORKS BASED ON TEST DATASET

Frameworks			True	
			Good	Bad
<b>Acoustic Only + KNN</b>	<b>Predicted</b>	Good	164	16
		Bad	15	35
<b>Acoustic Only + SVM</b>	<b>Predicted</b>	Good	161	9
		Bad	18	42
<b>Acoustic Only + RF</b>	<b>Predicted</b>	Good	166	12
		Bad	13	39
<b>PCA+KNN</b>	<b>Predicted</b>	Good	173	21
		Bad	6	30
<b>Acoustic and process parameters +KNN</b>	<b>Predicted</b>	Good	168	12
		Bad	11	39
<b>Acoustic and process parameters +SVM</b>	<b>Predicted</b>	Good	166	8
		Bad	13	43
<b>Acoustic and process parameters +RF</b>	<b>Predicted</b>	Good	173	10
		Bad	6	41

For future work, we seek to improve the performance of our proposed frameworks by adding more acoustic features and process parameters together. Also, we plan to characterize different print process parameters and explore their relationships with acoustic signals to enhance defect identification on our WAAM system further. Since our data set is not large enough to study the deep learning method that can directly extract the features. In the future, we plan to use other modalities and image-based data to explore deep learning methods.

## 6 Acknowledgement

The authors gratefully acknowledge the support of the ASTAR AME IAF-PP Grant number A19E1a0097.

## REFERENCES

- [1] Xu, F., Dhokia, V., Colegrove, P., McAndrew, A., Williams, S., Henstridge, A., and Newman, S. T., 2018. “Realisation of a multi-sensor framework for process monitoring of the wire arc additive manufacturing in producing ti-6al-4v parts”. *International Journal of Computer Integrated Manufacturing*, **31**(8), pp. 785–798.
- [2] Yuan, L., Pan, Z., Ding, D., He, F., van Duin, S., Li, H., and Li, W., 2020. “Investigation of humping phenomenon for the multi-directional robotic wire and arc additive manufacturing”. *Robotics and Computer-Integrated Manufacturing*, **63**, p. 101916.
- [3] Wu, B., Pan, Z., Ding, D., Cuiuri, D., Li, H., Xu, J., and Norrish, J., 2018. “A review of the wire arc additive manufacturing of metals: properties, defects and quality improvement”. *Journal of Manufacturing Processes*, **35**, pp. 127–139.
- [4] Xia, C., Pan, Z., Polden, J., Li, H., Xu, Y., Chen, S., and Zhang, Y., 2020. “A review on wire arc additive manufacturing: Monitoring, control and a framework of automated system”. *Journal of Manufacturing Systems*, **57**, pp. 31–45.
- [5] Wang, Y., and Zhao, P., 2001. “Noncontact acoustic analysis monitoring of plasma arc welding”. *International journal of pressure vessels and piping*, **78**(1), pp. 43–47.
- [6] Herala, A., 2012. *Monitoring and control of robotized laser metal-wire deposition*. Chalmers University of Technology.
- [7] Polajnar, I., Bergant, Z., and Grum, J., 2013. “Arc welding process monitoring by audible sound”. In 12th International Conference of the Slovenian Society for Non-Destructive Testing: Application of Contemporary Non-Destructive Testing in Engineering, ICNDT 2013-Conference Proceedings, pp. 613–20.
- [8] Pal, K., Bhattacharya, S., and Pal, S. K., 2010. “Investigation on arc sound and metal transfer modes for on-line monitoring in pulsed gas metal arc welding”. *Journal of Materials Processing Technology*, **210**(10), pp. 1397–1410.
- [9] Lv, N., Zhong, J., Chen, H., Lin, T., and Chen, S., 2014. “Real-time control of welding penetration during robotic gtaw dynamical process by audio sensing of arc length”. *The International Journal of Advanced Manufacturing Technology*, **74**(1-4), pp. 235–249.
- [10] Zhao, Y., Wang, J., Lu, Q., and Jiang, R., 2010. “Pattern recognition of eggshell crack using pca and lda”. *Innovative Food Science & Emerging Technologies*, **11**(3), pp. 520–525.
- [11] Yeo, C. Y., Al-Haddad, S., and Ng, C. K., 2011. “Animal voice recognition for identification (id) detection system”. In 2011 IEEE 7th International Colloquium on Signal Processing and its Applications, IEEE, pp. 198–201.
- [12] Whitaker, B. M., Suresha, P. B., Liu, C., Clifford, G. D., and Anderson, D. V., 2017. “Combining sparse coding and time-domain features for heart sound classification”. *Physiological measurement*, **38**(8), p. 1701.
- [13] Surovi, N. A., Dharmawan, A. G., and Soh, G. S., 2021. “A study on the acoustic signal based frameworks for the real-time identification of geometrically defective wire arc bead”. In International Design Engineering Technical Conferences and Computers and Information in Engineering Conference, Vol. 85383, American Society of Mechanical Engineers, p. V03AT03A003.
- [14] Madsen, P., 2005. “Marine mammals and noise: Problems with root mean square sound pressure levels for transients”. *The Journal of the Acoustical Society of America*, **117**(6), pp. 3952–3957.
- [15] Banchhor, S. K., and Khan, A., 2012. “Musical instrument recognition using zero crossing rate and short-time energy”. *Musical Instrument*, **1**(3), pp. 1–4.
- [16] Yao, P., and Zhou, K., 2017. “Application of short time energy analysis in monitoring the stability of arc sound signal”. *Measurement*, **105**, pp. 98–105.
- [17] Fan, D., Shi, Y., and Ushio, M., 2001. “Investigation of co welding arc sound: Correlation of welding arc sound signal with welding spatter (physics, processes, instruments & measurements)”. *Transactions of JWRI*, **30**(1), pp. 29–33.
- [18] Shahabi, H., and Kolahan, F., 2015. “Regression modeling of welded joint quality in gas metal arc welding process using acoustic and electrical signals”. *Proceedings of the Institution of Mechanical Engineers, Part B: Journal of Engineering Manufacture*, **229**(10), pp. 1711–1721.
- [19] Liu, L., Lan, H., Zheng, H., and Jian, X., 2012. “Feature extraction and dimensionality reduction of arc sound under typical penetration status in metal inert gas welding”. *Chinese Journal of Mechanical Engineering*, **25**(2), pp. 293–298.
- [20] Rabi, J., Balusamy, T., and Jawahar, R. R., 2019. “Analysis of vibration signal responses on pre induced tunnel defects in friction stir welding using wavelet transform and empirical mode decomposition”. *Defence Technology*, **15**(6), pp. 885–896.
- [21] Jalil, M., Butt, F. A., and Malik, A., 2013. “Short-time energy, magnitude, zero crossing rate and autocorrelation measurement for discriminating voiced and unvoiced segments of speech signals”. In 2013 The international conference on technological advances in electrical, electronics and computer engineering (TAAECE), IEEE, pp. 208–212.
- [22] Saini, D., and Floyd, S., 1998. “An investigation of gas

- metal arc welding sound signature for on-line quality control". *WELDING JOURNAL-NEW YORK*, **77**, pp. 172–s.
- [23] Zhao, S., Qiu, X., Burnett, I., Rigby, M., and Lele, A., 2019. "Statistical characteristics of gas metal arc welding (gmaw) sound". In Internatioanal Congress on Acoustics, EAA.
- [24] Lv, N., Xu, Y., Zhong, J., Chen, H., Wang, J., and Chen, S., 2013. "Research on detection of welding penetration state during robotic gtaw process based on audible arc sound". *Industrial Robot: An International Journal*.
- [25] Moser, M., 2014. *Engineering acoustics*. Springer.
- [26] Dinovitzer, M., Chen, X., Laliberte, J., Huang, X., and Frei, H., 2019. "Effect of wire and arc additive manufacturing (waam) process parameters on bead geometry and microstructure". *Additive Manufacturing*, **26**, pp. 138–146.
- [27] Ayed, A., Valencia, A., Bras, G., Bernard, H., Michaud, P., Balcaen, Y., and Alexis, J., 2020. "Effects of waam process parameters on metallurgical and mechanical properties of ti-6al-4v deposits". In *Advances in Materials, Mechanics and Manufacturing*. Springer, pp. 26–35.
- [28] Ortega, A. G., Galvan, L. C., Rouquette, S., and Deschaux-Beaume, F., 2017. "Effect of welding parameters on the quality of multilayer deposition of aluminum alloy". In Advances in Materials & Processing Technologies Conference.
- [29] Rosli, N. A., Alkahari, M. R., Ramli, F. R., Sudin, M. N., and Maidin, S., 2021. "Influence of process parameters in wire and arc additive manufacturing (waam) process". *Journal of Mechanical Engineering (JMechE)*, **17**(2), pp. 69–78.
- [30] Yaseer, A., and Chen, H., 2021. "Machine learning based layer roughness modeling in robotic additive manufacturing". *Journal of Manufacturing Processes*, **70**, pp. 543–552.
- [31] Xiong, J., Li, Y., Li, R., and Yin, Z., 2018. "Influences of process parameters on surface roughness of multi-layer single-pass thin-walled parts in gmaw-based additive manufacturing". *Journal of Materials Processing Technology*, **252**, pp. 128–136.
- [32] Rivero, D., Fernandez-Blanco, E., Dorado, J., and Pazos, A., 2011. "A new signal classification technique by means of genetic algorithms and knn". In 2011 IEEE Congress of Evolutionary Computation (CEC), IEEE, pp. 581–586.
- [33] Platt, J., et al., 1999. "Probabilistic outputs for support vector machines and comparisons to regularized likelihood methods". *Advances in large margin classifiers*, **10**(3), pp. 61–74.
- [34] Breiman, L., 2001. "Random forests". *Machine learning*, **45**(1), pp. 5–32.
- [35] Cawley, G. C., and Talbot, N. L., 2003. "Efficient leave-one-out cross-validation of kernel fisher discriminant classifiers". *Pattern Recognition*, **36**(11), pp. 2585–2592.
- [36] Provost, F., and Kohavi, R., 1998. "Glossary of terms". *Journal of Machine Learning*, **30**(2-3), pp. 271–274.